Available online at www.sciencedirect.com
ScienceDirect
Ceramics International 37 (2011) 105–110
CERAMICS INTERNATIONAL
www.elsevier.com/locate/ceramint

Effect of Ni substitution on electrical and thermoelectric properties of $LaCoO_3$ ceramics

Fu Li, Jing-Feng Li *

State Key Laboratory of New Ceramics and Fine Processing, Department of Materials Science and Engineering, Tsinghua University, Beijing 100084, China

Received 8 February 2010; received in revised form 10 June 2010; accepted 22 July 2010
Available online 22 August 2010

Abstract

$LaCo_{1-x}Ni_xO_3$ ($0 \leq x \leq 0.2$) ceramics were prepared by solid state reaction and their thermoelectric properties were investigated from room temperature (RT) to 400 °C. In the range from RT to 180 °C, $LaCoO_3$ showed a large negative Seebeck coefficient, but it changed to a positive value above 180 °C. However, the Seebeck coefficient became positive in the whole investigated temperature span due to Ni substitution for Co even for a tiny amount, but its absolute value decreased significantly with increasing Ni content. The $LaCo_{0.9}Ni_{0.1}O_3$ composition showed an enhanced power factor with a maximum value of 1.41×10^{-4} W m^{-1} K^{-2} at room temperature, which is about 3.5 times higher than that of un-doped $LaCoO_3$. Because the power factor decreased and the thermal conductivity increased apparently with temperature, the ZT values were not increased at elevated temperatures, in spite of a relatively large ZT value of 0.031 at a low temperature (50 °C) obtained in the composition $LaCo_{0.9}Ni_{0.1}O_3$.

Keywords: C. Electrical properties; C. Thermal properties; Lanthanum cobalt oxide; Thermoelectric properties

1. Introduction

Thermoelectric (TE) energy conversion is a promising technology for both electrical power generation in terms of waste heat recovery and various electronic cooling devices. The energy conversion efficiency of a TE device is mainly determined by the figure of merit (ZT) of its corresponding materials, which is expressed as $ZT = S^2\sigma T/\kappa$, where S, σ, κ and T are Seebeck coefficient, electrical conductivity, thermal conductivity, and absolute temperature, respectively. Therefore, good TE materials with a high ZT should have a high electrical conductivity σ, a high Seebeck coefficient S, and a low thermal conductivity κ. Although conventional TE compounds like Bi_2Te_3 possess high thermoelectric performance [1,2], they are easily decomposed or oxidized in air at high temperatures, whose applications are greatly limited [3]. Instead, oxide TE materials are relatively stable at high temperatures and receive recent attention in the fields of energy conversion [4–6].

Cobalt oxides are of particular interest as TE materials because of its large Seebeck coefficient and semiconducting or metallic electric conductivity [7–9]. They exhibit a strongly correlated electron system with Co ions presenting an energy level degeneracy of electronic states, which are considered as the origin of the large Seebeck coefficient at low temperatures. Lanthanum cobalt oxide ($LaCoO_3$) with a rhombohedra distorted perovskite structure provides a typical example for the thermally assisted spin state transition of the trivalent cobalt. It is possible to improve the Seebeck coefficient value and also to change its sign by suitable substitutions [10]. It was also reported that a low level La-site or Co-site substitution can improve its transport properties by changing the oxidation state of Co or by the formation of oxygen vacancies. Meanwhile, unlike the layered oxides, $LaCoO_3$ is isotropic, which may not require cumbersome technique of epitaxial growth when used for preparing thermoelectric devices [11]. Robert et al. [12,13] revealed that Ni substitution was an effective approach to enhance thermoelectric performance of $LaCoO_3$ ceramics, which motivated us to conduct the present study to attain a deeper understanding of the effect of Ni substitution. In this study, $LaCo_{1-x}Ni_xO_3$ ceramic samples were fabricated by a conventional solid state reaction and normal sintering method,

* Corresponding author. Tel.: +86 10 62784845; fax: +86 10 62771160.
E-mail address: jingfeng@mail.tsinghua.edu.cn (J.-F. Li).

0272-8842/$36.00
doi:10.1016/j.ceramint.2010.08.024

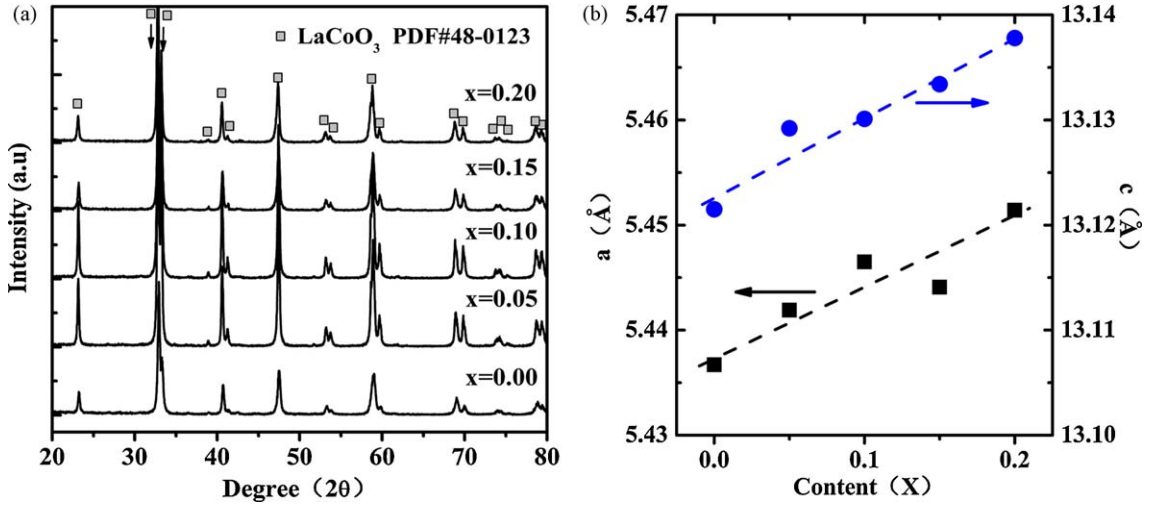

Fig. 1. XRD patterns (a) and lattice parameters (b) of $LaCo_{1-x}Ni_xO_3$ ($0 \le x \le 0.2$).

and the influence of Co substitution with Ni ions was studied by evaluation of electrical conductivity and Seebeck coefficient. It was found that the power factor at room temperature was significantly increased by only 10% Ni substitution to Co-site.

2. Experimental

$LaCo_{1-x}Ni_xO_3$ ($0 \le x \le 0.2$) samples were prepared by solid state reaction followed by normal sintering. Commercial powders of La_2O_3 (≥99.9%), Co_3O_4 (≥99.5%) and Ni_2O_3 (≥99.8%) were mixed according to the stoichiometric ratio in a ceramic jar with ceramic balls in acetone solution at 170 rpm for 20 h in a planetary ball mill. The well mixed powders were calcined at 1000 °C for 12 h in air and reground by ball milling for 3 h. Then, the resultant powders were compacted into disk-shaped samples ϕ15 mm in diameter and 3–4 mm in thickness, followed by sintering in air at 1200 °C for 12 h.

The densities of the samples were measured by the Archimedes method. The phase structures were investigated by X-ray diffraction (XRD) with a D/max-RB diffractometer (Rigaku, Tokyo, Japan) using CuK_α radiation. The polished surfaces of the sintered samples were thermally etched to show the grain boundaries for the observation of microstructure by field emission scanning electron microscopy (FE-SEM, LEO1530, Germany), the doped samples were thermally etched at 1050 °C for 30 min, while the un-doped ones were heated at 1100 °C for the same time. The Seebeck coefficient and electrical resistance data were recorded simultaneously as a function of temperature from 25 to 400 °C in a helium atmosphere using a Seebeck coefficient/electric resistance measuring system (ZEM-2, Ulvac-Riko, Japan). Within the same temperature range, the thermal diffusivity and the specific heat capacity were measured by a thermal conductivity measuring system (TC9000, Ulvac-Riko, Japan) and a differential scanning calorimeter (DSC-60, Shimadzu, Japan), respectively. Therefore, the thermal conductivity (k) was calculated from the thermal diffusivity (D) and the specific heat capacity (C_p) as well as the density (d), that is $k = DC_pd$.

3. Results and discussion

Fig. 1 shows the XRD patterns of the $LaCo_{1-x}Ni_xO_3$ samples. As compared with JCPDS data, the patterns of all the compositions can be indexed as a rhombohedra distorted perovskite structure, and no clear evidence of secondary phases was found. The present results are in accordance with the earlier investigations [12,13]. As shown in Fig. 1(b), the parameters linearly increase with increasing Ni substitution, confirming that the Ni ions entered into the $LaCoO_3$ lattices, since the ionic radius of Co^{3+} (0.063 nm) is smaller than that of Ni^{2+} (0.069 nm) [14].

Fig. 2. shows the SEM photographs of the polished and thermally etched surfaces of the samples with different compositions. The un-doped samples were dense with much larger crystalline grains about 3 μm. However, the grains of the Ni-substituted samples were about 300 nm, which are much smaller than that of the un-doped samples. This result indicates that Ni doping is effective to suppress the grain growth of $LaCoO_3$ ceramics. However, if compared with un-doped $LaCoO_3$, the grains in the Ni-substituted samples are not uniform with some fine grains around 50 nm particularly in the samples with low Ni contents. Nevertheless, such fine-grained microstructure is desirable for thermoelectric materials, whose thermal conductivity can be reduced by their enhanced phonon scattering due to the increased grain boundaries.

Fig. 3 shows the temperature dependences of Seebeck coefficients and electrical conductivity. At room temperature, the un-doped $LaCoO_3$ shows a large negative Seebeck coefficient. However, a small amount of Ni substitution changed the Seebeck coefficient from negative to positive sign with a large room-temperature positive Seebeck coefficient at $x = 0.05$. With increasing Ni content, however, the Seebeck coefficient decreased significantly, and the reasons will be discussed later. In the range of the investigated temperature, the sign of the value of all the Ni-substituted compounds was positive, being different from the un-doped $LaCoO_3$ sample, whose Seebeck coefficient showed a sign change around 180 °C, being similar to the

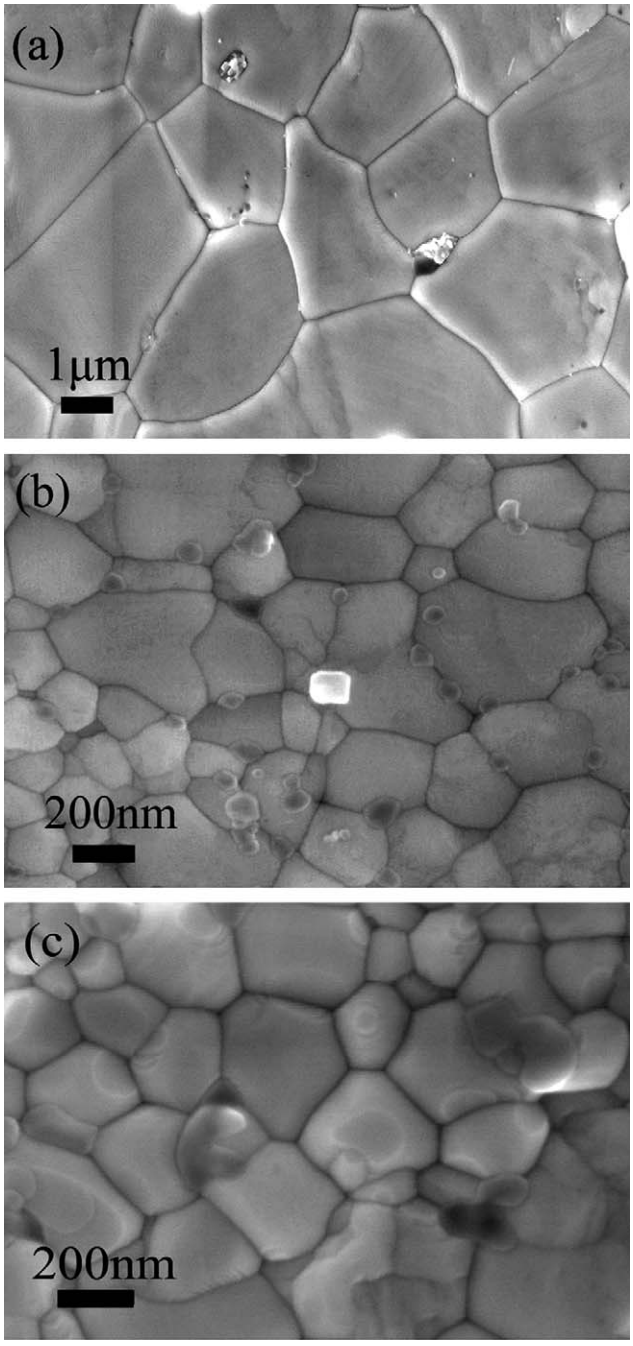

Fig. 2. SEM photographs of the sample surfaces (a) $LaCoO_3$, (b) $LaCo_{0.95}Ni_{0.05}O_3$ and (c) $LaCo_{0.8}Ni_{0.2}O_3$.

previous reports [15,16]. With increasing temperature, the absolute value of Seebeck coefficient for all Ni-substituted samples decreased.

$LaCoO_3$ exhibits quite peculiar magnetic and transport properties due to the 3d el9ectrons with a characteristic degeneracy as a result of spin and orbital degree of freedom. The Co^{3+} ions in the compound are in the low spin ground state configuration with $S = 0$ at room temperature, and then experience a transition to an intermediate $(t_{2g}^5 e_g^1)$ and to a high spin state $(t_{2g}^4 e_g^2)$ with increasing temperature. When the temperature is high enough, the Seebeck coefficient is expected to be determined by the so-called Heikes' equation [10,17]. The general expression has been expressed as:

$$S = -\frac{k_B}{e} \ln\left[\frac{g_3}{g_4}\frac{x}{1-x}\right] \quad (1)$$

where k_B is the Boltzmann's constant, and x is the concentration of Co^{4+} ions, g_3 and g_4 denote the degeneracy of Co^{3+} and Co^{4+}, respectively, in the octahedral coordination. This indicates that the absolute Seebeck coefficient depends on the degeneration of electronic states of Co^{3+} and Co^{4+} ions as well as the ratio between them [17,18]. In $LaCo_{1-x}Ni_xO_3$, the substitution of Co^{3+} by Ni^{3+} lead to an enhancement of the hole concentration and a reduction of the Seebeck coefficient. Therefore, it is inferred that Ni^{3+} turn to Ni^{2+} during sintering, since the latter is much stable at high temperatures in air [14]. The excess negative charge introduced by Ni^{2+} doping to $LaCoO_3$ is compensated either by creation of holes, that is, by the oxidation of Co^{3+} to Co^{4+}, or by creation of oxygen vacancies [19]. If the excess charge is compensated only by the oxidation of Co^{3+} to Co^{4+} and degeneration of electronic states between them is fixed at room temperature, then the Seebeck coefficient would decrease with increasing Ni content via Heikes' equation. With increasing temperature, the spin state transition and the ratio of Co^{3+} and Co^{4+} would be changed, causing the reduction of the Seebeck coefficient. When the temperature is above 327 °C, the spin state transition finishes and the newly formed holes introduced by doping dominate the transport term contributing to the Seebeck coefficient, causing a drop to a low value and being steady at high temperatures.

Fig. 3(b) shows the temperature dependence of the electrical conductivities of $LaCo_{1-x}Ni_xO_3$ compounds. All of the samples show semiconducting behavior in the measured temperature range as the electrical conductivity increases with increasing temperature. The substitution of Ni with Co causes a dramatic rise in the electrical conductivity, which increases from 1.32 to 55.3 S cm^{-1} at 50 °C when the Ni substitution is 20%. The improved electrical conductivity is due to the increased carrier concentration because of the substitution of Co^{3+} by Ni^{2+}. This is also related to the different band structure and the energy gap of the $LaCo_{1-x}Ni_xO_3$ compounds. If the mobile holes for the p-type semiconductors are small polarons, the electrical conductivity can be expressed as [20–22]:

$$\sigma = e\mu_p p \sim T^{-1} \exp\left(\frac{-E_a}{k_B T}\right) \quad (2)$$

where μ_p is the mobility of holes and E_a is the activation energy with $E_a = \Delta H_m + (E_g/2)$, where ΔH_m is the motional enthalpy of the holes. The plots of $\ln(\sigma T)$ versus $1/T$ for the $LaCo_{1-x}Ni_xO_3$ $(0 \le x \le 0.2)$ are displayed in Fig. 4. The E_a can be obtained form the plots. As seen from the curves, the data for the Ni-doped samples lie on a straight line, being indicative of hopping conduction. However, the line for undoped $LaCoO_3$ exhibits nonlinear variations in the whole temperature, suggesting a different conductive mechanism.

Temperature dependences of power factor (PF) are exhibited in Fig. 5. The PF of all the Ni-substituted compounds are larger

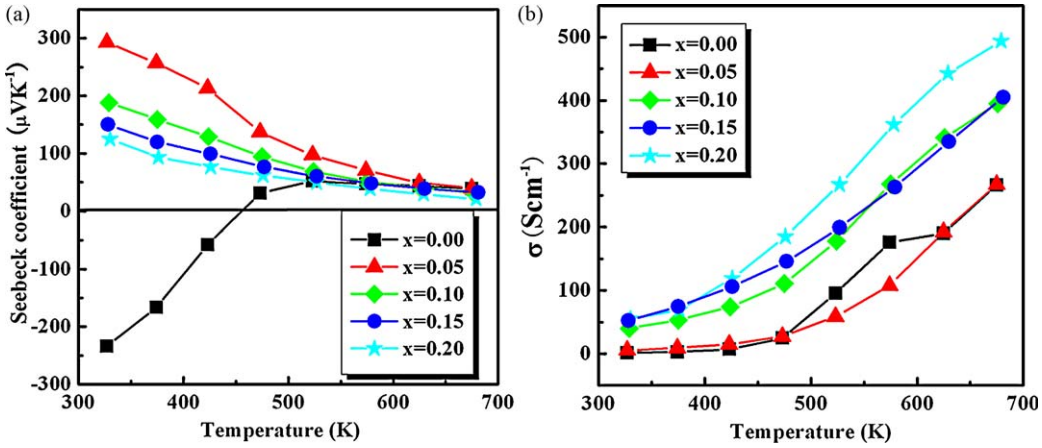

Fig. 3. Temperature dependences of the Seebeck coefficients (a) and the electrical conductivities (b) of $LaCo_{1-x}Ni_xO_3$ ($0 \le x \le 0.2$).

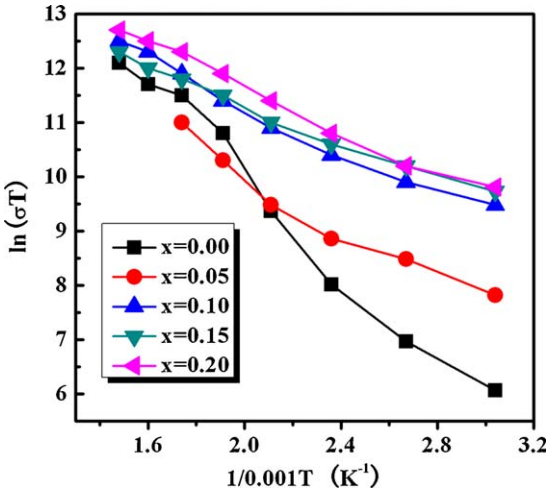

Fig. 4. Plots of $\ln(\sigma T)$ versus $1/T$ for $LaCo_{1-x}Ni_xO_3$ ($0 \le x \le 0.2$).

than that of un-doped $LaCoO_3$, and the $x = 0.10$ sample has a maximum PF of 1.41×10^{-4} W m^{-1} K^{-2} at 50 °C, being in concordance with the previous report, in which the compounds were prepared by soft chemistry process [13]. It should be noted that the PF value is much higher than that obtained in Ni and Sr doped $LaFeO_3$ [23]. However, the PF values decreased apparently when the Ni substitution exceeds $x = 0.10$, mainly because of the reduced Seebeck coefficient as shown in Fig. 3(a). Therefore, there exists an optimal Ni doping level to enhance the PF of $LaCo_{1-x}Ni_xO_3$.

Fig. 6 shows the temperature dependence of thermal diffusivity. It is clear that the samples with higher Ni contents have a larger value. However, the difference among the thermal diffusivity coefficients of the samples with Ni contents in the range of 0.05–0.15 is not so apparent at low temperature. The thermal conductivity, which is calculated from the thermal diffusivity and the specific heat capacity being consistent with the references [21] as well as the density measured by the Archimedes principle, are shown in Fig. 7. Around room temperature, the thermal conductivity of the un-doped samples is larger than that of the Ni-doped ones, which is a reasonable result because the former one has larger grain sizes than the latter as shown in Fig. 2. In addition, solid solution can effectively reduce thermal conductivity of the materials. As the temperature increases, the thermal conductivity increases apparently, particularly in the Ni-doped samples. The total thermal

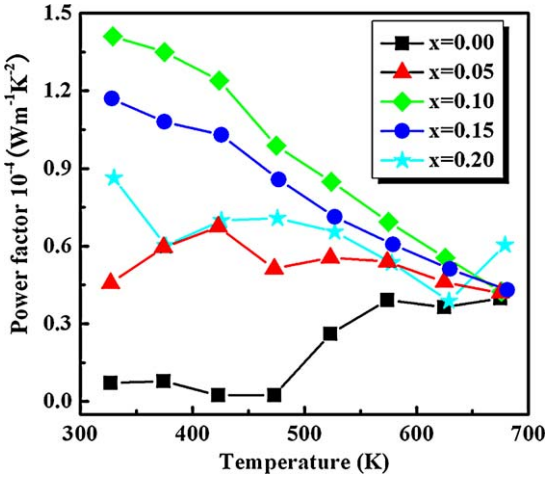

Fig. 5. Temperature dependences of the power factor of $LaCo_{1-x}Ni_xO_3$ ($0 \le x \le 0.2$).

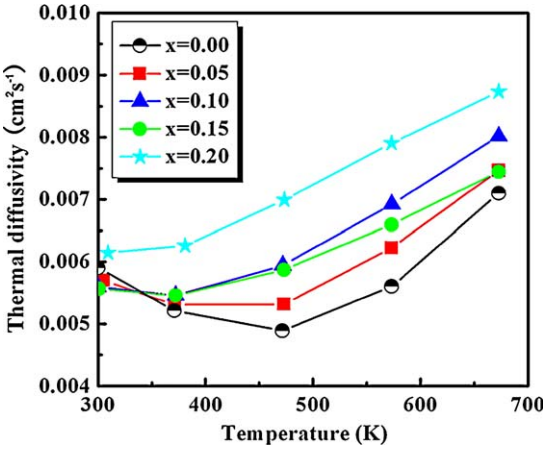

Fig. 6. Temperature dependences of thermal diffusivity of $LaCo_{1-x}Ni_xO_3$ ($0 \le x \le 0.2$).

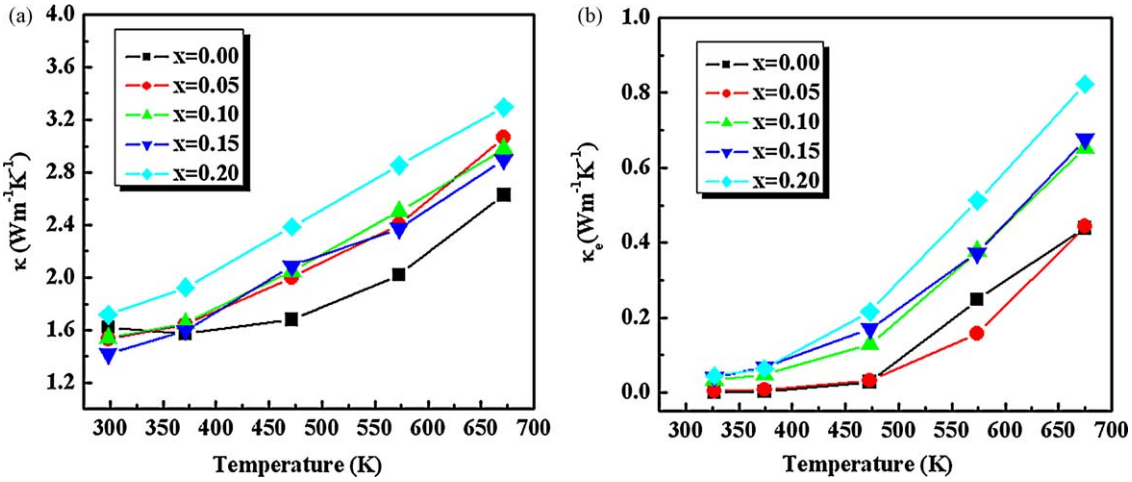

Fig. 7. Temperature dependences of thermal electric conductivity (a) and contribution of electrons of thermal conductivity (b) for the samples $LaCo_{1-x}Ni_xO_3$ ($0 \le x \le 0.2$).

conductivity can be expressed as $\kappa_t = \kappa_{ph} + \kappa_e$, where κ_{ph} is the phononic contribution and κ_e is the electronic contribution. When assuming the presence of the only one type of the charge carrier, being responsible for the electronic conduction, κ_e can be calculated using the Wiedemann–Franz–Lorenz relation, that is $\kappa_e = \sigma LT$, where L is Lorenz number. The obtained values are small especially at a lower temperature, $\le$8% of the total thermal conductivity which approximately increase to 20% at 673 K. This suggests that the heat is carried predominantly by phonon. For all the samples, κ_e increases with increasing temperature, as shown in Fig. 7(b), and the data of Ni-doped samples are larger than the un-doped one, except one point of the doped sample with the least content. This can be contributed to the increased current carrier concentration which is also in concordance with the electrical conductivity shown in Fig. 3(b). Few investigations were found reporting the thermal conductivity of $LaCoO_3$ polycrystalline materials. Robert et al. [12] reported an extremely low thermal conductivity reaching 0.44 W m^{-1} K^{-1} at room temperature, probably because their samples contained high porosity as the sintering temperature was as low as 1073 K. On the contrary, Androulakis et al. [11] reported a much higher room-temperature thermal conductivity up to 3.75 W m^{-1} K^{-1} in $La_{0.95}Sr_{0.05}CoO_3$ ceramic samples than that shown by the present materials. Nevertheless, the thermal conductivity obtained in the present study is relatively low as for oxide materials, which can be attributed to the fine-grained microstructure as shown in Fig. 2.

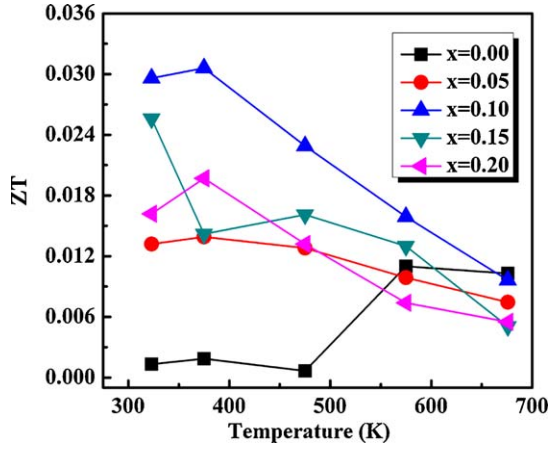

Fig. 8. Temperature dependence of ZT value of $LaCo_{1-x}Ni_xO_3$ ($0 \le x \le 0.2$).

The calculated figure of merit, ZT, is shown in Fig. 8. The maximum ZT value is 0.031 at 50 °C for the 10% doped sample, which is higher than the reported value of ZT = 0.022 [24]. However, it is considerably lower than the value ZT = 0.2 reported by Robert et al. [12], but their maximum ZT value corresponds to a much lower thermal conductivity (0.44 W m^{-1} K^{-1}) with an additional influence of porosity as mentioned above. Therefore, there is room to further increase the ZT values of $LaCo_{1-x}Ni_xO_3$ ceramics by taking nanostructuring measures to reduce thermal conductivity.

4. Conclusions

$LaCo_{1-x}Ni_xO_3$ ($0 \le x \le 0.2$) oxide ceramics were prepared by conventional solid state reaction and normal sintering. The samples show dense and fine-grained microstructure of a single phase with perovskite structure. It is found that the substitution of Co with Ni in $LaCoO_3$ increases the electrical conductivity significantly, but reduces the Seebeck coefficient. As a result, the power factor was optimized when the amount of Ni substitution was around 10%. The maximum room-temperature power factor obtained in $LaCo_{0.9}Ni_{0.1}O_3$ is 1.41×10^{-4} W m^{-1} K^{-2}, which is above 3 times higher than that (0.4×10^{-4} W m^{-1} K^{-2}) of $LaCoO_3$. It also shows that the doped element is effective to suppress the grain growth of $LaCoO_3$ ceramics, which can reduce the thermal conductivity at room temperature. Therefore, enhanced ZT values were obtained in the composition $LaCo_{0.9}Ni_{0.1}O_3$ with a maximum of 0.031 at 50 °C. The ZT values were not increased at elevated temperatures, because the power factor decreases and the thermal conductivity increases apparently with temperature. As the result reveals an intrinsic correlation between transport behavior and thermoelectric response, the thermoelectric properties can be improved by choosing suitable substitution with a proper doping content and

by controlling the crystal structure factors in such a strongly correlated electron system with transition metals.

Acknowledgements

The work was supported by the National Basic Research Program of China (Grant No. 2007CB607500) and National Nature Science Foundation (Grant No. 50820145203) as well as Tsinghua University Initiative Scientific Research Program.

References

[1] B. Poudel, Q. Hao, Y. Ma, Y.C. Lan, A. Minnich, B. Yu, X. Yan, D.Z. Wang, A. Muto, D. Vashaee, X.Y. Chen, J.M. Liu, M.S. Dresselhaus, G. Chen, Z. Ren, High-thermoelectric performance of nanostructured bismuth antimony telluride bulk alloys, Science 320 (2008) 634–638.

[2] J.F. Li, J. Liu, Effect of nano-SiC dispersion on thermoelectric properties of Bi_2Te_3 polycrystals, Physica Status Solidi A: Applications and Materials Science 203 (2006) 3768–3773.

[3] M. Shikano, R. Funahashi, Electrical and thermal properties of single-crystalline $(Ca_2CoO_3)_{(0.7)}CoO_2$ with a $Ca_3Co_4O_9$ structure, Applied Physics Letters 82 (2003) 1851–1853.

[4] Y. Wang, Y. Sui, J. Cheng, X.J. Wang, J.P. Miao, Z.G. Liu, Z.N. Qian, W.H. Su, High temperature transport and thermoelectric properties of Ag-substituted $Ca_3CO_4O_{9+delta}$ system, Journal of Alloys and Compounds 448 (2008) 1–5.

[5] R. Funahashi, S. Urata, Fabrication and application of an oxide thermoelectric system, International Journal of Applied Ceramic Technology 4 (2007) 297–307.

[6] H. Cheng, X.J. Xu, H.H. Hng, J. Ma, Characterization of Al-doped ZnO thermoelectric materials prepared by RF plasma powder processing and hot press sintering, Ceramics International 35 (2009) 3067–3072.

[7] I. Terasaki, Y. Sasago, K. Uchinokura, Large thermoelectric power in $NaCo_2O_4$ single crystals, Physical Review B 56 (1997) 12685–12687.

[8] A. Maignan, S. Hebert, L. Pi, D. Pelloquin, C. Martin, C. Michel, M. Hervieu, B. Raveau, Perovskite manganites and layered cobaltites: potential materials for thermoelectric applications, Crystal Engineering 5 (2002) 365–382.

[9] Y.F. Zhang, J.X. Zhang, Q.M. Lu, Synthesis of highly textured $Ca_3Co_4O_9$ ceramics by spark plasma sintering, Ceramics International 33 (2007) 1305–1308.

[10] A. Maignan, D. Flahaut, S. Hebert, Sign change of the thermoelectric power in $LaCoO_3$, European Physical Journal B 39 (2004) 145–148.

[11] J. Androulakis, P. Migiakis, J. Giapintzakis, $La_{0.95}Sr_{0.05}CoO_3$: an efficient room-temperature thermoelectric oxide, Applied Physics Letters 84 (2004) 1099–1101.

[12] R. Robert, L. Bocher, B. Sipos, M. Dobeli, A. Weidenkaff, Ni-doped cobaltates as potential materials for high temperature solar thermoelectric converters, Progress in Solid State Chemistry 35 (2007) 447–455.

[13] R. Robert, L. Bocher, M. Trottmann, A. Reller, A. Weidenkaff, Synthesis and high-temperature thermoelectric properties of Ni and Ti substituted $LaCoO_3$, Journal of Solid State Chemistry 179 (2006) 3893–3899.

[14] I. Alvarez, J.L. Martínez, M.L. Veiga, C. Pico, Synthesis, structural characterization, and electronic properties of the $LaNi_{1-x}W_xO_3$ $(0 \leq x \leq 0.25)$ perovskite-like system, Journal of Solid State Chemistry 125 (1996) 47–53.

[15] T Ohtani, K. Kuroda, K. Matsugami, D. Katoh, Electrical resistivity and thermopower of $(La_{1-x}Sr_x)MnO_3$ and $(La_{1-x}Sr_x)CoO_3$ at elevated temperatures, Journal of the European Ceramic Society 20 (2000) 2721–2726.

[16] T. He, J.Z. Chen, T.G. Calvarese, M.A. Subramanian, Thermoelectric properties of $La_{(1-x)}A_{(x)}CoO_{(3)}$ (A = Pb, Na), Solid State Sciences 8 (2006) 467–469.

[17] P.M. Chaikin, G. Beni, Thermopower in correlated hopping regime, Physical Review B 13 (1976) 647–651.

[18] W. Koshibae, K. Tsutsui, S. Maekawa, Thermopower in cobalt oxides, Physical Review B 62 (2000) 6869–6872.

[19] A. Mineshige, M. Kobune, S. Fujii, Z. Ogumi, M. Inaba, T. Yao, K. Kikuchi, Metal–insulator transition and crystal structure of $La_{1-x}Sr_xCoO_3$ as functions of Sr-content, temperature, and oxygen partial pressure, Journal of Solid State Chemistry 142 (1999) 374–381.

[20] A.J Zhou, T.J. Zhu, X.B. Zhao, H.Y. Chen, E. Muller, Fabrication and thermoelectric properties of perovskite-type oxide $La_{1-x}Sr_xCoO_3$ ($x = 0$, 0.1), Journal of Alloys and Compounds 449 (2008) 105–108.

[21] M.A. Senarisrodriguez, J.B. Goodenough, $LaCoO_3$ revisited, Journal of Solid State Chemistry 116 (1995) 224–231.

[22] M.A. Senarisrodriguez, J.B. Goodenough, Magnetic and transport-properties of the system $La_{1-x}Sr_xCoO_{3\text{-}delta}$ (0-less-than-x-less-than-or-equal-to-0.50), Journal of Solid State Chemistry 118 (1995) 323–336.

[23] K. Iwasaki, T. Ito, M. Yoshino, T. Matsui, T. Nagasaki, Y. Arita, Power factor of $La_{1-x}Sr_xFeO_3$ and $LaFe_{1-y}Ni_yO_3$, Journal of Alloys and Compounds 430 (2007) 297–301.

[24] P. Migiakis, J. Androulakis, J. Giapintzakis, Thermoelectric properties of $LaNi_{1-x}Co_xO_3$ solid solution, Journal of Applied Physics 94 (2003) 7616–7620.